IEEE Access
Multidisciplinary | Rapid Review | Open Access Journal

Received 10 March 2023, accepted 4 April 2023, date of publication 7 April 2023, date of current version 13 April 2023.

Digital Object Identifier 10.1109/ACCESS.2023.3265587

RESEARCH ARTICLE

Multi-Feed Metasurface Antennas: Direct Numerical Design and Experimental Validations

MODESTE BODEHOU[1], (Member, IEEE), ADRIEN GUTH[2], KHALDOUN AL KHALIFEH[1], (Member, IEEE), DIRK HEBERLING[2], (Senior Member, IEEE), AND CHRISTOPHE CRAEYE[1], (Senior Member, IEEE)

[1]ICTEAM Institute, Université catholique de Louvain, 1348 Louvain-la-Neuve, Belgium
[2]Institute of High Frequency Technology, RWTH Aachen University, 52074 Aachen, Germany

Corresponding author: Modeste Bodehou (modeste.bodehou@uclouvain.be)

This work was supported by the Belgian Fonds National de la Recherche Scientifique, Chargé de Recherche Program.

ABSTRACT This paper provides new designs and realizations of leaky-wave (LW) metasurface (MTS) antennas fed at multiple points. The design technique is based on the direct integral-equation solution by the Method of Moments (MoM). The unknown is no longer the current distribution, but the impedance profile itself. The method can be used to generate any shaped radiation pattern in amplitude, phase, and polarization, provided that the antenna area and the feeder illumination are consistent with the shape of the desired radiation pattern. The algorithm can also be used to design multi-functional antennas (multibeam, multiband, dual-polarizion, etc). While multiple feeds are traditionally used to implement multiple fonctionnalities, they may also be required for the efficient generation of a single shaped beam, thus leading to a higher surface-wave (SW) to LW conversion efficiency. The present paper shows for the first time, two realizations of MTS design with the integral equation formalism, which require the usage of multiple feeds: a circularly polarized sectoral conical beam and a dual-polarized broadside beam MTS antenna. The good comparison between measurements and numerical predictions shows the effectiveness of the design method.

INDEX TERMS Metasurfaces, leaky-wave antennas, shaped beams, dual-polarization.

I. INTRODUCTION

Surface-wave (SW) based metasurface (MTS) antennas have been extensively studied in the previous decade given the various advantages offered by this technology [1], [2], [3], [4], [5], [6], [7], [8], [9], [10], [11], [12], [13]: high gain, low-profile including the feeder, low power losses, simple fabrication process, etc. Those advantages make the MTS technology very attractive in many communication and radar applications, both terrestrial and in space. The design principles of SW based MTS antennas have been first inspired by the work of Oliner and Hessel [1], in which the authors demonstrated that a sinusoidally modulated reactance surface can serve as a leaky-wave radiator. The first practical realization of this concept has been provided by Fong et al. [2]. Radiation originates from the interference between a transverse-magnetic (TM) SW with an inductive impenetrable surface impedance. The latter has been realized with sub-wavelength patches printed on a grounded slab. The control of the polarization of the beam using the holographic method has been demonstrated in [3], [4], and [5].

Over the past few years, a rich progress has been made in this field. Analytical solutions of the surface impedance have been proposed in [6] for the generation of pencil beams. Extensions to shaped beams synthesis have been provided in [7] and [8], using semi-analytical methods based on a locally sinusoidal approximation. In particular, [8] has introduced a synthesis approach based on Flat-optics, which allows for a local control of the leakage rate and the phase progression of the SW over the aperture. Several realizations

The associate editor coordinating the review of this manuscript and approving it for publication was Bilal Khawaja.

based on the Flat optics, including the generation of multiple beams, have been reported in [9]. The Flat optics approach has also been used in [10] for the generation of vortex beams. Pencil beams scanning versus frequency has been achieved in [11] using a SW reflector, and a similar functionality is demonstrated in [12] with 1D leaky-wave antenna based on substrate integrated waveguide.

Recently, a different approach, directly inspired from the Method of Moments (MoM), has been proposed [13], [14], [15], [16], [17]. The MoM is a well known numerical technique for the analysis of radiation and scattering problems through the solution of a surface integral equation [18]. The latter stems from two theoretical principles. First, the scattered fields are expressed as the convolution of the surface currents with the Green's function (field radiated by a point source current). Second, the discretized currents are obtained through the enforcement of the boundary conditions. Effective MTS antenna analysis tools based on the MoM have been proposed in [19], [20], [21], [22], and [23]. Those tools rely on the homogenization of the MTS, i.e. a modeling of the cladding with an equivalent sheet impedance distribution [24]. The latter relates the average electric field at the MTS to the surface current flowing on the cladding.

The direct integral equation-based MTS synthesis relies on the same principle as the MoM. However, instead of expanding an unknown surface current, here the surface-current is assumed to be known. The unknown now is the MTS impedance distribution, which is expanded into a set of basis functions. The coefficients of expansion are found after directly solving the integral equation. Thereafter, other methods for the optimization of MTS antennas, not based on local periodicity assumption, have been proposed in [25] and [26] and so far numerically demonstrated for 2D pencil beams. The advantages of the direct integral equation method w.r.t. the literature are multiple. First, the design method enables taking directly as input, the desired radiation pattern and does not require a definition of the leakage rate or the propagating wave constant as is traditionally the case when designing leaky-wave antennas. Second, the class of impedance profiles that can be generated is general (not necessarily locally sinusoidal), while being very smooth at the sub-wavelength scale to ease the implementation in terms of sub-wavelength patches. Third, an unprecedented control of the 3D radiation pattern (in amplitude, phase, and polarization) or the antenna near-field can be achieved within a reasonable computation time (less than 30 min on a conventional laptop computer).

An important evolution regarding MTS antennas concerns the use of multiple feeds to either achieve better efficiency for 3D shaped beam generation [17] or to allow the generation of several beams from a single aperture [9], [15], [16]. The contributions of this paper consist of experimentally demonstrating such functionalities using the integral equation-based design method. In the first example, multiple feeds have been used simultaneously to generate a single shaped beam with good efficiency, i.e. the feeder illumination profile is adapted to the radiated aperture field so as to prevent the surface-wave (SW) from reaching the rim in weakly modulated sectors of the antenna. In the second example, multiple feeds are used to generate two broadside pencil beams with orthogonal circular polarizations, while preserving the simplicity of the feeder.

The paper is structured as follows. Section II briefly recalls the synthesis method, Section III provides the experimental validations and Section IV concludes the paper.

II. MTS ANTENNA DESIGN BASED ON INTEGRAL EQUATION SOLUTION

A. INTEGRAL EQUATION FORMULATION

Let us consider a modulated capacitive sheet impedance laying on a grounded slab, as represented in Fig. 1.

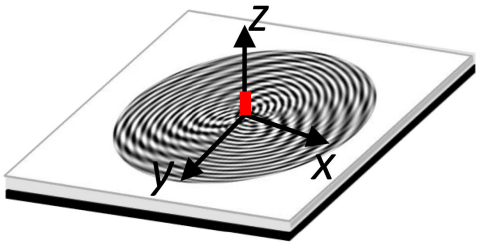

FIGURE 1. A MTS antenna illustration.

The MTS is fed by a SW lancher, usually a simple monopole. We assume an anisotropic and lossless sheet impedance $\mathbf{Z}_S$ of the form:

$$\begin{aligned} Z_S^{\rho\rho}(\rho,\phi) &= Z_0 + P^{\rho\rho}(\rho,\phi) \\ Z_S^{\rho\phi}(\rho,\phi) &= Z_S^{\phi\rho}(\rho,\phi) = P^{\rho\phi}(\rho,\phi) \\ Z_S^{\phi\phi}(\rho,\phi) &= Z_0 - P^{\rho\rho}(\rho,\phi) \end{aligned} \tag{1}$$

where Z_0 is the average impedance over which the surface impedance is modulated, and $P^{\rho\rho}$ and $P^{\rho\phi}$ describe the modulation at the point of cylindrical coordinates (ρ,ϕ). The surface impedance $\mathbf{Z}_S$ linearly relates the tangential electric field $\mathbf{E}_t$ to the surface current $\mathbf{J}$ over the aperture, i.e. $\mathbf{E}_t = \mathbf{Z}_S \,.\, \mathbf{J}$. Therefore, the surface current and the surface impedance satisfy the following electric field integral equation (EFIE) [24]:

$$\hat{\mathbf{z}} \times \left[\iint_{S'} \mathbf{G}^{EJ}(\boldsymbol{\rho}, \boldsymbol{\rho}')\, \mathbf{J}(\boldsymbol{\rho}')\, dS' - \mathbf{Z}_S(\boldsymbol{\rho})\, \mathbf{J}(\boldsymbol{\rho}) \right] = -\hat{\mathbf{z}} \times \mathbf{E}_i \tag{2}$$

where $\hat{\mathbf{z}}$ is the unit vector normal to the surface, $\mathbf{G}^{EJ}$ is the dyadic spatial Green's function providing the field generated at a position $\boldsymbol{\rho}$ by a point source current placed at $\boldsymbol{\rho}'$ and $\mathbf{E}_i$ is the antenna excitation field.

As explained in [13], expanding the surface current and the surface impedance into a set of basis functions, enables after Galerkin testing the numerical derivation of the surface impedance from the required current distribution. However, because of the a priori lack of the near-field knowledge, the non-radiating spectrum of the current should be guessed from

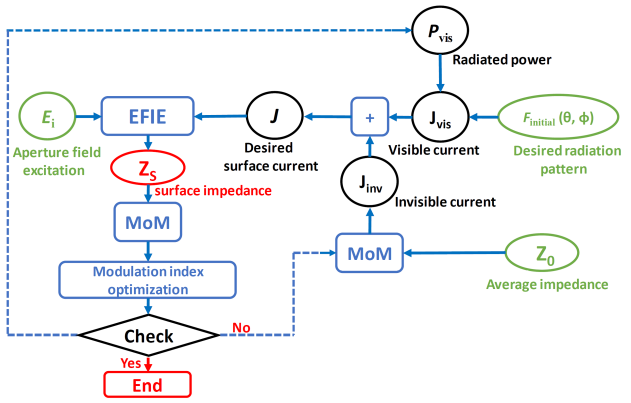

FIGURE 2. Flowchart of the metasurface synthesis method. $F_{initial}(\theta, \phi)$ is the desired radiation pattern, and E_i is the aperture electric field corresponding to the antenna excitation. J_{vis} is the desired visible current, and J_{inv} is an estimate of the invisible current. Z_S is the synthesized surface impedance. Details regarding each block of the flowchart can be found in [13], [14].

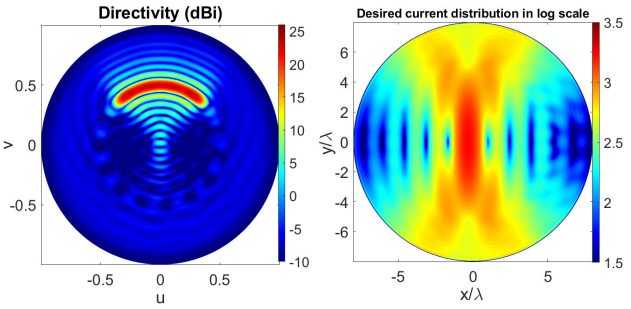

FIGURE 3. Right-hand circularly polarized sectoral conical beam. a) illustration in the u-v plane. b) Absolute value of the desired current distribution.

the one corresponding to the average reactance surface. The absence of losses in the surface impedance is imposed in the least-squares sense, while solving the EFIE. The modulation depth is thereafter optimized to achieve a good compromise between the aperture efficiency and the conversion efficiency [14]. The conversion efficiency (ϵ_{conv}) is defined as the ratio between the radiated power, assuming an infinitely extended grounded slab, and the power provided by the feeder [27]. A second iteration may be eventually carried out based on a first design, from which the new estimate of the non-radiating part of the current is taken, as well as the feeding power. The feeding power can be computed using the algorithms proposed in [27] and [28]. The synthesis method is summarized in Fig. 2.

B. FEEDER DESIGN

The design technique explained previously assumes the knowledge of the aperture field $\mathbf{E}_i$ generated by the feeder (see equation (2)). Usually, the feed is a simple monopole placed at the center of the antenna. While this feeder choice is well adapted to the generation of pencil beams, it is not necessarily a good choice for a certain class of shaped beams.

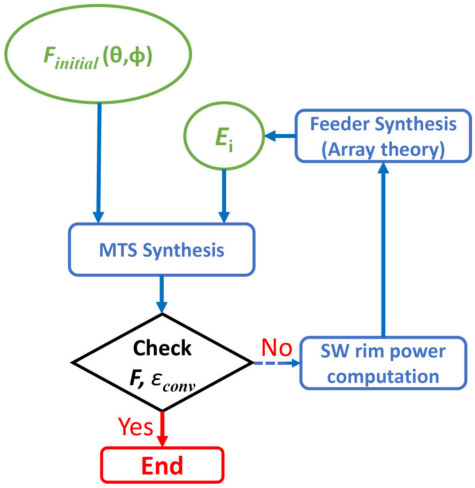

FIGURE 4. Block diagram of the algorithm. $F_{initial}(\theta, \phi)$ is the desired radiation pattern, and E_i is the aperture electric field corresponding to the antenna excitation. F is the obtained radiation pattern after MTS synthesis, and ϵ_{conv} stands for the conversion efficiency. ϵ_{conv} can be computed with the algorithms proposed in [27], [28].

Indeed, as demonstrated in [17], the desired radiation pattern may translate into a strong variation of the amplitude of the radiating aperture field (or current distribution) along the azimuth direction. As an example, the desired radiating current distribution required to generate a sectoral conical beam (see Fig. 3(a)) is represented in Fig. 3(b). This type of beams can be used for radar observation to focus the radiated power on an a priori known azimuthal sector of observation. It can be seen that the left and right parts of the antenna radiate much less than the top and bottom parts. The SW power launched by the feed in the less radiating portions of the aperture will not significantly leak before reaching the rim of the antenna, thus limiting the conversion efficiency ($\epsilon_{conv} < 50\%$ for the example in Fig. 3). This rim SW power is then diffracted in an uncontrolled fashion, leading to high sidelobes. This problem can be solved by designing the feed so as to illuminate less the weakly radiating portions of the antenna. More precisely, the feeder illumination along azimuth should be approximately proportional to the desired radiating power along azimuth. A simple way to achieve this goal consists of using an array of monopoles properly fed in phase and amplitude [17]. The resulting synthesis method can be summarized as follows. First a single monopole placed at the center is used to feed the antenna, and the design is carried out accordingly [13], [14]. In case the obtained conversion efficiency is not satisfactory, the SW power reaching the rim is computed (for example with the method proposed in [27]) and the feeder is designed to generate an azimuth illumination inversely proportional to the SW rim power. The array feeding design can be carried out using well known antenna array synthesis techniques (see for example chapter 10 of [29] and references therein). The MTS is thereafter redesigned with the updated feed. The algorithm is schematically represented in Fig. 4.

C. MULTI-FUNCTIONAL DESIGN

The synthesis method also enables the design of multi-functionnal antennas (e.g. multibeam with multiple feeds, multiband, etc). In that case, one should simply concatenate the equations associated with each feed, and corresponding radiation pattern and frequency, and solve the resulting system of equations in the least-squares sense as already done in [16]. It is worth mentioning that, contrary to the array feeder designed to maximize the conversion efficiency (Section II-B), in the multi-functional case, the feeders are usually separated by more than one wavelength. Nevertheless, both techniques can be combined to generate multiple shaped beams. The design of two sectoral conical beams with four monopoles has been shown in [17]. Each beam is generated by activating an array of two electrically close monopoles.

III. EXPERIMENTAL RESULTS

This section provides two realizations of MTS antennas design with the integral-equation based method. In the first example, the aperture is shared by two feeds activated simultaneously to provide a right handed circularly polarized sectoral conical beam as represented in Fig. 3(a). The second antenna is a dual-polarized MTS antenna. The two antennas have been designed at 24 GHz with the substrate Rogers4350B of relative permittivity $\epsilon_r = 3.66$ and thickness 1.524 mm, and we have chosen an average reactance of $X_0 = -772\ \Omega$.

A. SECTORAL CONICAL BEAM

As explained in Section II-B, generating the sectoral conical beam with a very good conversion efficiency requires the usage of an array of two monopole feeders. Indeed, using a single monopole, the conversion efficiency is limited to about 45%, while the usage of two monopoles allows one to exceed 80% [17]. Two monopole feeds are placed at $(x = -0.17\lambda,\ y = 0)$ and $(x = 0.17\lambda,\ y = 0)$, where λ is the free-space wavelength. The monopoles are fed simultaneously with the same amplitude and phase. The synthesized surface impedance is illustrated in Fig. 5. The antenna is circular with a radius equal to 8λ. It provides a peak directivity of 21.7 dBi, while the desired peak directivity is 23.4 dBi.

This surface impedance has been implemented with coffee bean patches (illustrated in Fig. 6a of [14]) periodically arranged using a square unit cell of size $\lambda/7$ using the same procedure as in [14]. The realized antenna is shown in Fig. 6.

A 2-ways high power Wilkinson power divider has been used to feed the two monopoles in phase. The measured normalized directivity is compared with simulation results of the surface impedance in Figs. 7(a)-(e). The simulations of the surface impedance have been carried out with a MoM code based on Fourier-Bessel basis functions (FBBF) [20].

It can be seen that there is a good agreement between simulated patterns obtained with the designed surface impedance

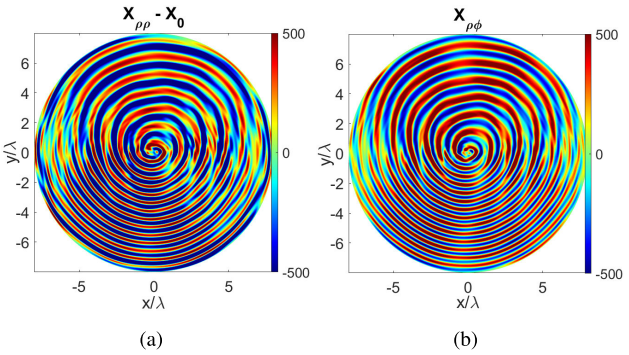

FIGURE 5. Reactance modulation required to generate the circularly polarized sectoral conical beam.

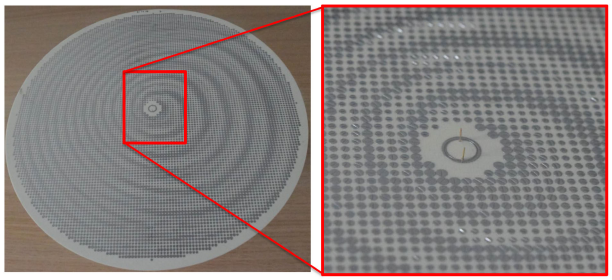

FIGURE 6. Picture of the fabricated sectoral conical beam MTS antenna.

and the measured patterns. The predicted co-polarized sidelobe level is similar to the one obtained from measurements, which indicates a good conversion efficiency for this antenna. The 3D radiation pattern is illustrated in Fig. 8. The measured gain is 20 dBi, which compares well with the expected directivity (21.7 dBi). The differences can be attributed to the error made during the surface impedance implementation process, and to Ohmic losses. In the future, a full-wave code capable of analyzing the fine physical structure of the MTS should be developed to address that issue. The cross-pol level can be improved by better optimizing the modulation depth of each component of the anisotropic modulation as done in [28]. The measured reflection coefficient ($S11$) is shown in Fig. 9 and is equal to -11 dB at 24 GHz. This reflection coefficient can be refined by adapting the length of the pin. It has not been done here because the process is sensitive and shortening a thin pin is not reversible. It is worth mentioning that the matching can be carried out almost independently to the MTS design as demonstrated in [28] and does not constitute a challenge for this type of antennas as long as the feed is fabricated with a good precision.

B. DUAL-POLARIZED MTS ANTENNA

Dual-polarized antennas can find applications in MIMO communications to exploit the polarization diversity or for multiplexing over orthogonal polarizations [31]. They can also be used for radar polarimetry [32], and space communication and sensing. Dual-polarized MTS antennas have already been designed in the literature based on the simultaneous

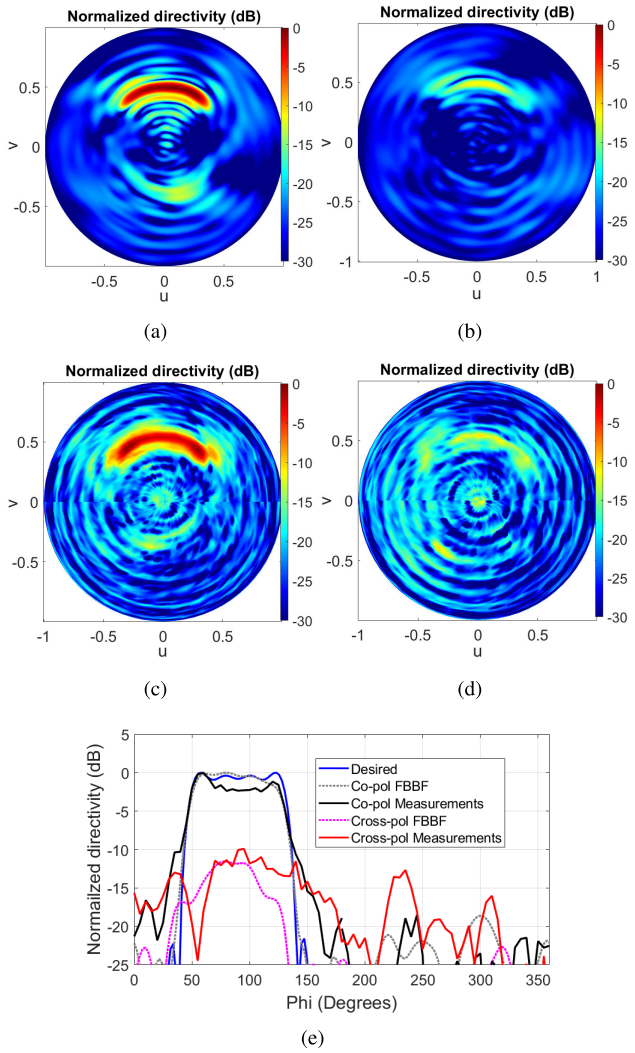

FIGURE 7. Numerical and experimental results for the designed circularly polarized sectoral conical beam. (a) Co-pol normalized directivity from the FBBF simulation. (b) Cross-pol normalized directivity from the FBBF simulation. (c) Measured Co-pol normalized directivity. (d) Measured Cross-pol normalized directivity. (e) Comparison of the directivities in the cone $\theta = 30^o$.

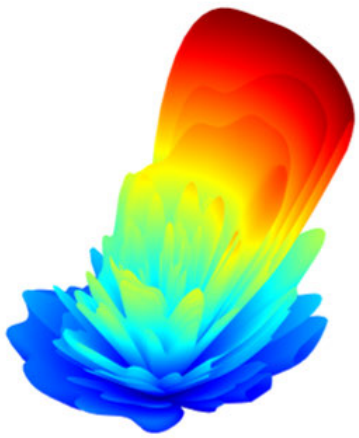

FIGURE 8. 3D representation of the radiation pattern of the sectoral conical beam antenna.

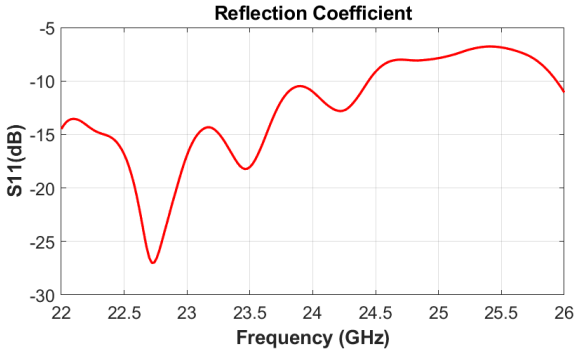

FIGURE 9. Measured reflection coefficient of the sectoral conical beam antenna shown in Fig. 6.

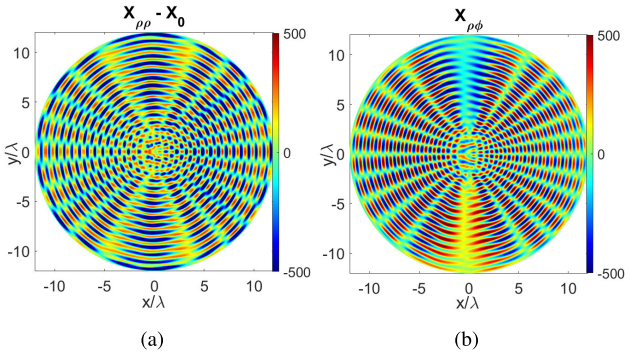

FIGURE 10. Reactance modulation designed for a dual-polarized MTS antenna.

excitation of TM and TE SWs [4], [30]. The advantage of the solution proposed here mainly lies in the simplicity of the feeding structure and the achievable bandwidth, given that our antenna is excited with TM SW feeders only, meaning that the propagating SW mode is dominantly TM. The antenna radius is fixed to 12λ. The MTS is designed to provide at 24 GHz a right-handed circularly polarized (RHCP) broadside beam using a monopole feeder placed at $(x = 0, y = 2\lambda)$, and a left-handed circularly polarized (LHCP) broadside beam with a monopole feeder placed at $(x = 0, y = -2\lambda)$. The obtained surface impedance is shown in Fig. 10.

Square unit cells of size $\lambda/10$ have been used for the surface impedance implementation. Given the fabrication constraints on the minimum admissible distance between two metallizations (100 μm), anisotropic reactances close to zero ($X \in [-200\ \Omega,\ 0]$) have not been well implemented, which implies a limitation of the effectively implemented modulation depth as compared to the synthesized one. This problem can be overcome by investigating other patch shapes. The realized antenna is shown in Fig. 11.

Due to the electrically large antenna size, the measurements have been carried out in the Compact Antenna Test Range of the Institute of High Frequency Technology of

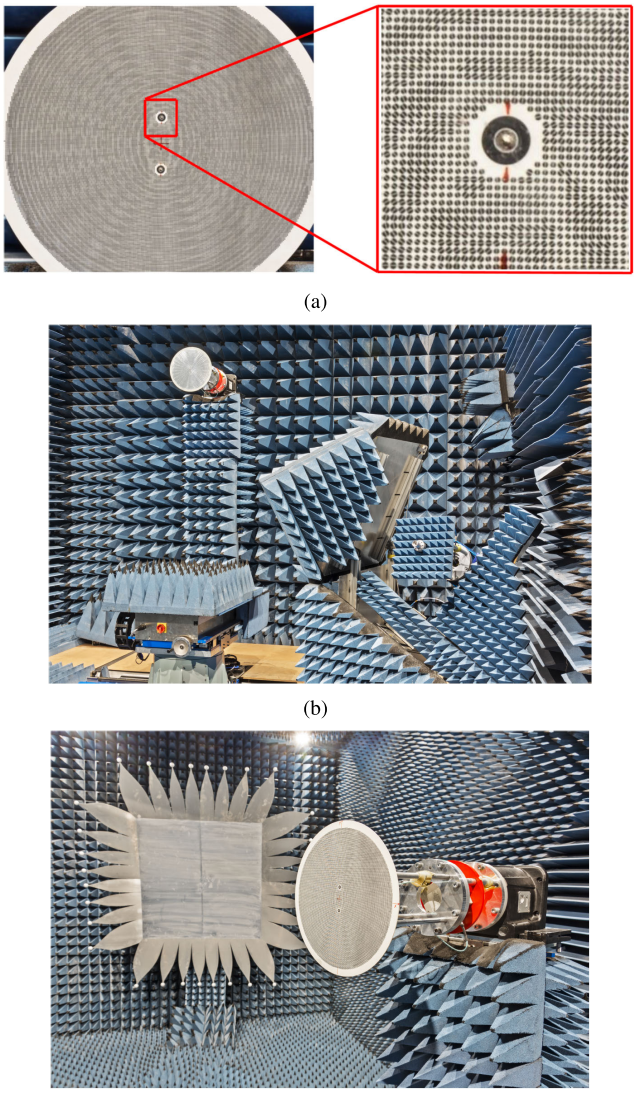

(a) (b) (c)

FIGURE 11. Realized dual-polarized MTS antenna along with the measurement setup.

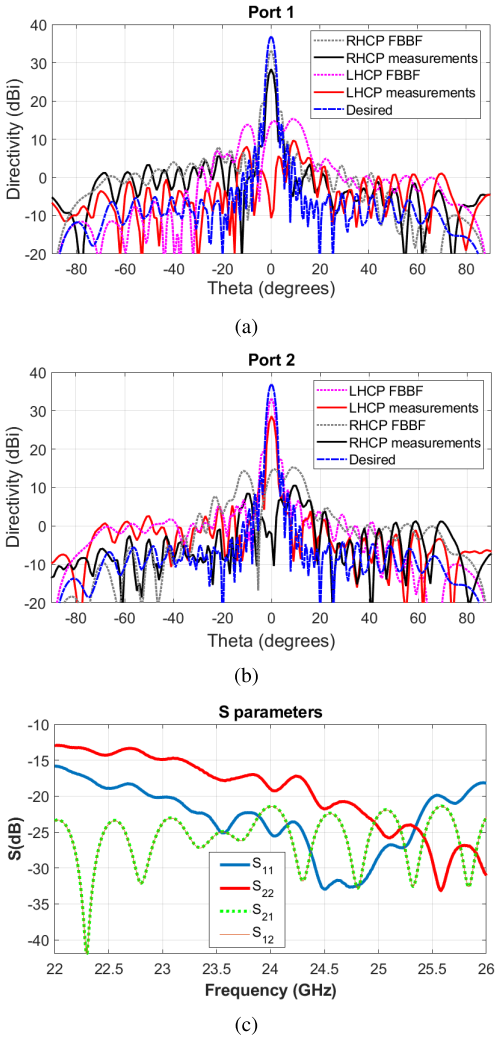

(a) (b) (c)

FIGURE 12. Characterization of dual-polarized broadside beam MTS antenna. a) Directivity corresponding to the first feed. b) Directivity corresponding to the second feed. c) Measured S parameters at the antenna ports. The difference between the predicted directivity and the measured one can be explained by the limited conversion efficiency (55%) after surface impedance implementation, given the fabrication constraints, and the inaccuracy of the surface impedance implementation.

the RWTH Aachen University. The measurement setup comprises a feed antenna (on the side), a parabolic reflector and a roll-over-azimuth positioner. The spherical waves emitted by the feed illuminate the reflector and are collimated into a plane wave by the reflector's shape. The MTS mounted on the positioner is located in the measurement chamber's quiet zone (QZ). The QZ is defined as a cylindrical region of 1.2 m diameter, where the plane wave is specified in terms of amplitude taper and phase ripple. This configuration allows direct characterization in the far field of the MTS. Simulated and measured radiation patterns are compared in Fig. 12. The simulation of the effectively realized surface impedance (taking into account the limitation of the coffee beans and fabrication constraints) predicts a directivity of 33 dBi, corresponding to an aperture efficiency of 34%. However, the numerically predicted conversion efficiency is 55%, mainly because the implemented modulation depth has been limited by fabrication constraints. Therefore the total efficiency (product between the aperture and conversion efficiencies) is 19% only. The inaccuracy in the surface impedance implementation and the resulting limited conversion efficiency (55%) are the main reasons for the difference between the predicted directivity and the obtained one. Indeed, the simulations assume an infinitely extended slab. As a consequence, diffraction at the rim due to the truncation of the slab is not modeled. In that case, if the conversion efficiency is not sufficiently high, the SW is not well attenuated before reaching the rim. Therefore, it continues to propagate in the infinite slab and does not appear in the radiation pattern. In practice, the truncation of the slab leads to diffraction of the SW at the rim, producing higher sidelobes than expected, thus deteriorating the directivity. That is the reason why one

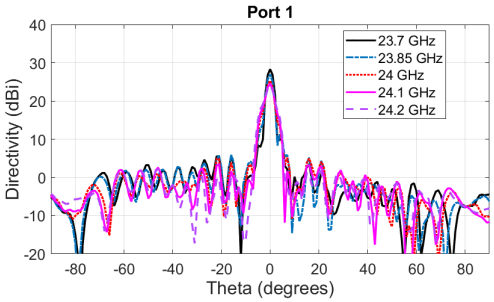

(a)

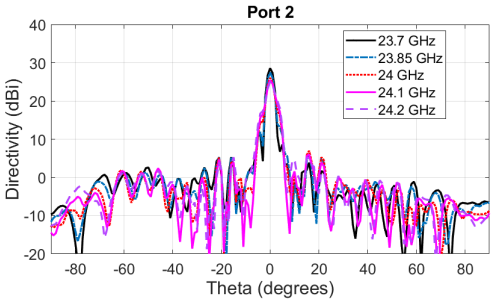

(b)

FIGURE 13. Directivity versus frequency of the dual-polarized antenna. The operating frequency of the realized dual-polarized antenna is slightly shifted to 23.7 GHz, probably due to fabrication tolerance issues.

should improve as best as possible the conversion efficiency to limit the undesired rim diffraction effects. It is precisely for this purpose that an array of two monopoles has been used in the first realized antenna (Section III-A) to generate a single shaped beam.

It has also been observed that the operating frequency of the realized dual-polarized antenna is slightly shifted to 23.7 GHz (see Fig. 13), probably due to fabrication tolerance issues. The measured directivity is 28.4 dBi, corresponding to an aperture efficiency of 12.1%. The measured cross-pol level is very good, i.e. −30 dB lower than the co-pol, which is significantly better than the numerically predicted cross-pol level. In comparison, [30] has reported an aperture efficiency of 18.2% for the first feed, and 13.5% for the second feed with a cross-pol level at −25 dB. However, the antenna, and in particular the feeding system in [30] is much more complex than that of the present paper because a simultaneous and well balanced excitation of the TE and TM modes is required by [30]. The measured 3dB beam bandwidth of our antenna is 3.4% and the antenna is well matched in the frequency band of interest (see Fig. 12(c)). The directivity can be improved by properly optimizing the modulation depth as done in [28], followed by a more accurate implementation of the surface impedance. This will also require a full-wave analysis of the physical structure of the MTS, which has not been done here because of the large size of the antenna. The array feeder solution used in the example of Section III-A may also be envisaged here to better improve the conversion efficiency. But the feeder will be more complex (more elements in the array) than in the first example, because the non-modulated sectors of the antenna are intertwined with the well modulated sectors. A compromise should be found between complexity and performance. Finally, it is worth mentioning that multiband synthesis with one or multiple feeds can be handled with the direct integral equation based method as demonstrated in [15].

IV. CONCLUSION

Metasurface antennas present the great advantage of being flat, while allowing complex radiation patterns. This allows placing the antennas on walls, ceilings, vehicles, while being practically invisible when illuminating prescribed surfaces, either for communication or radar purposes. A direct numerical design method of metasurface antennas with multiple feeds has been presented and experimentally validated. The method starts from the specifications of the radiation pattern, in amplitude, phase and polarization and the aperture field excitation. From there, the surface impedance is derived after solving numerically an electric field integral equation (EFIE). Two realizations have been provided. In the first example, multiple feeds have been simultaneously used to generate effectively a single shaped beam. Owing to the usage of two feeds, the conversion efficiency of the antenna has been significantly improved (from 45% to 80%). In the second experimental example, multiple feeds are used to generate beams with orthogonal polarizations. The innovation here relies on the generation of two beams with orthogonal circular polarizations (RHCP versus LHCP), while maintaining the simplicity of the feeding system. The measurements of the realized antennas demonstrate the capability of the synthesis method to control the shape and the polarization of the radiation pattern, as well as the capability to generate multiple functionalities with a single MTS platform. Future work should address the efficient full-wave analysis of metasurface antennas in order to account for the impact of limited fabrication tolerance.

REFERENCES

[1] A. A. Oliner and A. Hessel, "Guided waves on sinusoidally-modulated reactance surfaces," *IRE Trans. Antennas Propag.*, vol. 7, no. 5, pp. 201–208, Dec. 1959.

[2] B. H. Fong, J. S. Colburn, J. J. Ottusch, J. L. Visher, and D. F. Sievenpiper, "Scalar and tensor holographic artificial impedance surfaces," *IEEE Trans. Antennas Propag.*, vol. 58, no. 10, pp. 3212–3221, Oct. 2010.

[3] S. Pandi, C. A. Balanis, and C. R. Birtcher, "Design of scalar impedance holographic metasurfaces for antenna beam formation with desired polarization," *IEEE Trans. Antennas Propag.*, vol. 63, no. 7, pp. 3016–3024, Jul. 2015.

[4] M. Li, S.-Q. Xiao, and D. F. Sievenpiper, "Polarization-insensitive holographic surfaces with broadside radiation," *IEEE Trans. Antennas Propag.*, vol. 64, no. 12, pp. 5272–5280, Dec. 2016.

[5] A. Amini, H. Oraizi, M. Hamedani, and A. Keivaan, "Wide-band polarization control of leaky waves on anisotropic holograms," *Phys. Rev. Appl.*, vol. 13, no. 1, Jan. 2020, Art. no. 014038.

[6] G. Minatti, M. Faenzi, E. Martini, F. Caminita, P. De Vita, D. González-Ovejero, M. Sabbadini, and S. Maci, "Modulated metasurface antennas for space: Synthesis, analysis and realizations," *IEEE Trans. Antennas Propag.*, vol. 63, no. 4, pp. 1288–1300, Apr. 2015.

[7] M. Teniou, H. Roussel, N. Capet, G.-P. Piau, and M. Casaletti, "Implementation of radiating aperture field distribution using tensorial metasurfaces," *IEEE Trans. Antennas Propag.*, vol. 65, no. 11, pp. 5895–5907, Nov. 2017.

[8] G. Minatti, F. Caminita, E. Martini, M. Sabbadini, and S. Maci, "Synthesis of modulated-metasurface antennas with amplitude, phase, and polarization control," *IEEE Trans. Antennas Propag.*, vol. 64, no. 9, pp. 3907–3919, Sep. 2016.
[9] M. Faenzi, G. Minatti, D. González-Ovejero, F. Caminita, E. Martini, C. D. Giovampaola, and S. Maci, "Metasurface antennas: New models, applications and realizations," *Sci. Rep.*, vol. 9, no. 1, pp. 1–14, Jul. 2019.
[10] A. Amini and H. Oraizi, "Control of orbital angular momentum regimen by modulated metasurface leaky-wave antennas," *IEEE Trans. Antennas Propag.*, vol. 70, no. 11, pp. 10166–10176, Nov. 2022.
[11] A. M. Hakimi, A. Keivaan, H. Oraizi, and A. Amini, "Wide-scanning circularly polarized reflector-based modulated metasurface antenna enabled by a broadband polarizer," *IEEE Trans. Antennas Propag.*, vol. 70, no. 1, pp. 84–96, Jan. 2022.
[12] P. Sohrabi, P. Rezaei, S. Kiani, and M. Fakhr, "A symmetrical SIW-based leaky-wave antenna with continuous beam scanning from backward-to-forward through broadside," *Wireless Netw.*, vol. 27, no. 8, pp. 5417–5424, Nov. 2021.
[13] M. Bodehou, C. Craeye, E. Martini, and I. Huynen, "A quasi-direct method for the surface impedance design of modulated metasurface antennas," *IEEE Trans. Antennas Propag.*, vol. 67, no. 1, pp. 24–36, Jan. 2019.
[14] M. Bodehou, K. Alkhalifeh, S. N. Jha, and C. Craeye, "Direct numerical inversion methods for the design of surface wave-based metasurface antennas: Fundamentals, realizations, and perspectives," *IEEE Antennas Propag. Mag.*, vol. 64, no. 4, pp. 24–36, Aug. 2022.
[15] M. Bodehou, C. Craeye, and I. Huynen, "Multifrequency band synthesis of modulated metasurface antennas," *IEEE Antennas Wireless Propag. Lett.*, vol. 19, no. 1, pp. 134–138, Jan. 2020.
[16] M. Bodehou, E. Martini, S. Maci, I. Huynen, and C. Craeye, "Multibeam and beam scanning with modulated metasurfaces," *IEEE Trans. Antennas Propag.*, vol. 68, no. 3, pp. 1273–1281, Mar. 2020.
[17] M. Bodehou and C. Craeye, "Array surface-wave launcher for the efficient generation of shaped beam and multibeam with metasurface," *IEEE Trans. Antennas Propag.*, vol. 69, no. 12, pp. 8860–8865, Dec. 2021.
[18] R. F. Harrington, *Field Computation by Moment Method*. Piscataway, NJ, USA: IEEE Press, 1993.
[19] D. González-Ovejero and S. Maci, "Gaussian ring basis functions for the analysis of modulated metasurface antennas," *IEEE Trans. Antennas Propag.*, vol. 63, no. 9, pp. 3982–3993, Sep. 2015.
[20] M. Bodehou, D. González-Ovejero, C. Craeye, and I. Huynen, "Method of moments simulation of modulated metasurface antennas with a set of orthogonal entire-domain basis functions," *IEEE Trans. Antennas Propag.*, vol. 67, no. 2, pp. 1119–1130, Feb. 2019.
[21] M. Bodehou, C. Craeye, H. Bui-Van, and I. Huynen, "Fourier–Bessel basis functions for the analysis of elliptical domain metasurface antennas," *IEEE Antennas Wireless Propag. Lett.*, vol. 17, no. 4, pp. 675–678, Apr. 2018.
[22] F. Vernì, M. Righero, and G. Vecchi, "On the use of entire-domain basis functions and fast factorizations for the design of modulated metasurface," *IEEE Trans. Antennas Propag.*, vol. 68, no. 5, pp. 3824–3833, May 2020.
[23] J. Cavillot, M. Bodehou, S. Hubert, and C. Craeye, "Efficient analysis of planar, arbitrarily shaped, and (Bi)-anisotropic metasurface antennas," *IEEE Trans. Antennas Propag.*, vol. 70, no. 1, pp. 536–546, Jan. 2022.
[24] M. A. Francavilla, E. Martini, S. Maci, and G. Vecchi, "On the numerical simulation of metasurfaces with impedance boundary condition integral equations," *IEEE Trans. Antennas Propag.*, vol. 63, no. 5, pp. 2153–2161, May 2015.
[25] S. Pearson and S. V. Hum, "Optimization of electromagnetic metasurface parameters satisfying far-field criteria," *IEEE Trans. Antennas Propag.*, vol. 70, no. 5, pp. 3477–3488, May 2022.
[26] J. Budhu, L. Szymanski, and A. Grbic, "Design of planar and conformal, passive, lossless metasurfaces that beamform," *IEEE J. Microw.*, vol. 2, no. 3, pp. 401–418, Jul. 2022.
[27] M. Bodehou, D. González-Ovejero, C. Craeye, S. Maci, I. Huynen, and E. Martini, "Power balance and efficiency of metasurface antennas," *Sci. Rep.*, vol. 7, pp. 1–11, Jan. 2020.
[28] J. Cavillot, M. Bodehou, and C. Craeye, "Metasurface antennas design: Full-wave feeder modeling and far-field optimization," *IEEE Trans. Antennas Propag.*, vol. 71, no. 1, pp. 39–49, Jan. 2023.
[29] P.-S. Kildal, *Foundations of Antenna Engineering: A Unified Approach for Line-of-Sight and Multipath*, Hardcover, Ed. 2015. [Online]. Available: https://www.amazon.com/Foundations-Antenna-Engineering-Line-Sight/dp/B01GLEB19C
[30] A. T. Pereda, F. Caminita, E. Martini, I. Ederra, J. Teniente, J. C. Iriarte, R. Gonzalo, and S. Maci, "Experimental validation of a Ku-band dual-circularly polarized metasurface antenna," *IEEE Trans. Antennas Propag.*, vol. 66, no. 3, pp. 1153–1159, Mar. 2018.
[31] C. Oestges, B. Clerckx, M. Guillaud, and M. Debbah, "Dual-polarized wireless communications: From propagation models to system performance evaluation," *IEEE Trans. Wireless Commun.*, vol. 7, no. 10, pp. 4019–4031, Oct. 2008.
[32] A. Bhattacharya, S. Dey, and A. C. Frery, "Scattering purity and complexity in radar polarimetry," *IEEE Trans. Geosci. Remote Sens.*, vol. 60, 2022, Art. no. 5222514.

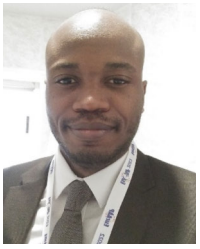

MODESTE BODEHOU (Member, IEEE) was born in Cotonou, Benin, in 1992. He received the B.Sc. degree in engineering and the M.Sc. degree in electrical engineering (telecommunications) from the Royal Military Academy, Brussels, Belgium, in 2013 and 2015, respectively, and the Ph.D. degree in engineering and technology and the master's degree in management from the Université catholique de Louvain, Louvain-la-Neuve, Belgium, in 2020 and 2022, respectively.

In 2015, he was with the Quartier Major Housiau (Belgium Defense), Vilvoorde, Belgium, where he was involved in the framework of his application school on military communication systems. He is currently an FNRS Postdoctoral Researcher with the Microwave and Applied Electromagnetism Laboratory, Université catholique de Louvain. His current research interests include computational electromagnetics, antenna arrays, and metasurfaces.

Dr. Bodehou was a recipient of the 2021 EurAAP Per-Simon Kildal Award for the Best Ph.D. in Antennas and Propagation, the Best Student Paper Award from the 13th European Conference on Antennas and Propagation, Krakow, Poland, 2019, the First Prize Student Paper Competition Award from the IEEE-MTT International Conference on Numerical Electromagnetic and Multiphysics Modeling and Optimization for RF, Microwave, and Terahertz Applications, Seville, Spain, 2017, and the AIA Price for the Best Engineering Master Thesis Award from the Royal Military Academy, Brussels, Belgium, 2015.

ADRIEN GUTH was born in Bonn, Germany, in 1993. He received the B.Sc. and M.Sc. degrees in electrical engineering from RWTH Aachen University, Aachen, Germany, in 2016 and 2019, respectively. Since 2019, he has been a Research Assistant and a Doctoral student with the Institute of High Frequency Technologies, RWTH Aachen University. His current research interests include spherical near-field antenna measurements and phaseless near-field measurements.

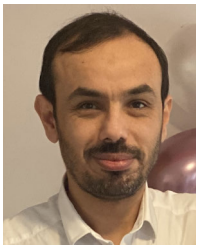

KHALDOUN AL KHALIFEH (Member, IEEE) was born in Aleppo, Syria. He received the Diploma in electrical and electronic engineering from Aleppo University-Faculty of Electrical and Electronic Engineering, in 2006, the master's degree in microwave and telecommunication from the Université catholique de Louvain (UCL), Belgium, in 2010, and the Ph.D. degree in applied sciences from UCL, in March 2017. From 2011 to 2017, he was a Research Assistant with the Antenna Research Group, Institute of Information and Communication Technologies, Electronics and Applied Mathematics (ICTEAM), Universite catholique de Louvain. Since 2020, he has been a Postdoctoral Researcher UCL. His research interests include multiband antenna array design and analysis, ground-penetrating radar (GPR) applications, space applications, fast numerical methods for electromagnetic fields in finite periodic structures, near-field imaging, and meta-surface antennas.

DIRK HEBERLING (Senior Member, IEEE) received the Dipl.-Ing. degree in electrical engineering and the Dr.-Ing. degree for his thesis on conformal microstrip antennas from RWTH Aachen University, Aachen, Germany, in 1987 and 1993, respectively.

From 1987 to 1993, he was a Scientist with the Institute for RF-Technologies, RWTH Aachen University. In 1993, he joined IMST GmbH, Kamp-Lintfort, Germany, to establish a new Antenna Section, and from 1995 to 2003, he was the Head of the Antennas Department, which was reorganized into the Department of Antennas and EMC, in 1998. From 2003 to 2008, he took over the Department of Information and Communication Systems, IMST GmbH. In 2008, he joined RWTH Aachen University, where he is currently the Head of the Institute and holds the Chair for High Frequency Technology. In 2016, he became the Director of the Fraunhofer Institute for High Frequency Physics and Radar Techniques, FHR, Munich, Germany. He is a member of VDE. Since 1998, he has been a member of the ITG Expert Group 7.1 Antennen, which he directed as a Chairperson, from 2002 to 2003, and since 2014, he has been responsible as the General Chairperson and an Organizer of the International Antenna Conference INICA 2003, Berlin, and the German Microwave Conference GeMiC 2014, Aachen. Since 1998, he has been a member of the European competence projects for antennas COST 260, COST 284, IC0603, and IC1102. From 2002 to 2007, he was the German delegate of COST 284. He is currently the German delegate of IC1102. From 2002 to 2003, he was a Co-Organizer of the European Network of Excellence on Antennas ACE. He is a member of the steering committee and organizing committee for the European Conference on Antennas and Propagation. Since 2015, he has been a member of the Board of Directors of the Antenna Measurement Techniques Association. He was elected to the technical decision board (Fachkollegiat) of the German Research Foundation DFG.

CHRISTOPHE CRAEYE (Senior Member, IEEE) was born in Belgium, in 1971. He received the Electrical Engineering and B.Phil. degrees from the Université catholique de Louvain (UCLouvain), Louvain-la-Neuve, Belgium, and the Ph.D. degree in applied sciences from UCLouvain, in 1994 and 1998, respectively.

From 1994 to 1999, he was a Teaching Assistant with UCLouvain and carried out research on the radar signature of the sea surface perturbed by rain, in collaboration with NASA and ESA. From 1999 to 2001, he was a Postdoctoral Researcher with the Eindhoven University of Technology, Eindhoven, The Netherlands. He was with the University of Massachusetts, Amherst, MA, USA, in 1999. He was with the Netherlands Institute for Research in Astronomy, Dwingeloo, The Netherlands, in 2001. In 2002, he started an antenna research activity with UCLouvain, where he is currently a Professor. He was with the Astrophysics and Detectors Group, University of Cambridge, Cambridge, U.K., in 2011. His research was funded by the Region Wallonne, European Commission, ESA, FNRS, and UCLouvain. His current research interests include mutual coupling, finite antenna arrays, wideband antennas, small antennas, metamaterials, fast physical optics, and numerical methods for fields in periodic media, with applications to communication and sensing systems.

Dr. Craeye received the 2005–2008 Georges Vanderlinden Prize from the Belgian Royal Academy of Sciences, in 2009. He was an Associate Editor of the IEEE TRANSACTIONS ON ANTENNAS AND PROPAGATION, from 2004 to 2010, and the IEEE ANTENNAS AND WIRELESS PROPAGATION LETTERS, from 2011 to 2017.